Sgk3 links growth factor signaling to maintenance of progenitor cells in the hair follicle

Laura Alonso,[1] Hitoshi Okada,[2] Hilda Amalia Pasolli,[1] Andrew Wakeham,[2] Annick Itie You-Ten,[2] Tak W. Mak,[2,3,4] and Elaine Fuchs[1]

[1]Laboratory of Mammalian Cell Biology and Development, Howard Hughes Medical Institute, The Rockefeller University, New York, NY 10021
[2]The Campbell Family Institute for Breast Cancer Research/Ontario Cancer Institute, University Health Network, Toronto, Ontario M5G 2M9, Canada
[3]Department of Medical Biophysics and [4]Department of Immunology, University of Toronto, Toronto, Ontario M5G 2C1, Canada

Tyrosine kinase growth factor receptor signaling influences proliferation, survival, and apoptosis. Hair follicles undergo cycles of proliferation and apoptotic regression, offering an excellent paradigm to study how this transition is governed. Several factors are known to affect the hair cycle, but it remains a mystery whether Akt kinases that are downstream of growth factor signaling impact this equilibrium. We now show that an Akt relative, Sgk (serum and glucocorticoid responsive kinase) 3, plays a critical role in this process. Hair follicles of mice lacking Sgk3 fail to mature normally. Proliferation is reduced, apoptosis is increased, and follicles prematurely regress. Maintenance of the pool of transiently amplifying matrix cells is impaired. Intriguingly, loss of Sgk3 resembles the gain of function of epidermal growth factor signaling. Using cultured primary keratinocytes, we find that Sgk3 functions by negatively regulating phosphatidylinositol 3 kinase signaling. Our results reveal a novel and important function for Sgk3 in controlling life and death in the hair follicle.

Introduction

Tissue homeostasis relies on a delicate balance of proliferation and apoptosis. Understanding the molecular mechanisms that are involved is a prerequisite for learning how the process goes awry in disease states, including cancers as well as autoimmune and inflammatory disorders. The murine hair follicle is a dynamic model of coordinated cell division, differentiation, and cell death that provides an effective platform for investigating the regulation of proliferation and apoptosis.

During embryonic hair follicle development, mesenchymal condensates assemble beneath the epidermis and induce downward epithelial remodeling and proliferation to form a hair bud (Schmidt-Ullrich and Paus, 2005). As the follicle develops, daughter cells within the central core begin to exit the cell cycle and differentiate to generate the hair shaft and its surrounding channel, the inner root sheath (IRS). By the time the follicle reaches maturity shortly after birth, it has established a remarkably productive hair factory, called the bulb, that contains transiently proliferative epithelial (matrix) cells surrounding specialized mesenchymal cells (dermal papilla [DP]) at the base. The matrix cells differentiate upward into six lineage-distinct, concentric cellular layers of the hair shaft and IRS.

After the growth phase, the follicle suddenly undergoes a catastrophic arrest, during which time the lower two thirds recedes; some cells terminally differentiate, and others undergo apoptosis (Muller-Rover et al., 2001). As the residual strand of epithelial cells shrinks, the mature mesenchymal condensate (DP) is dragged upward until it comes to rest below the permanent epithelial portion of the follicle. The mesenchymal–epithelial interaction stimulates activation of stem cells, and a new hair growth cycle begins (Taylor et al., 2000; Blanpain et al., 2004; Morris et al., 2004). Cycles of growth (anagen), regression (catagen), and rest (telogen) continue throughout the lifetime of all mammalian hair follicles. Despite the temporally discrete phases of proliferation and apoptosis in the hair follicle, little is known about the signals that maintain proliferation and/or cell survival during anagen, and even less is known about how these signals are balanced against those that promote catagen.

Numerous studies encompassing many different eukaryotic systems underscore the importance of tyrosine kinase growth factor receptor signaling pathways in regulating proliferation, survival, differentiation and apoptosis (for review see

L. Alonso and H. Okada contributed equally to this work.

Correspondence to Elaine Fuchs: fuchslb@rockefeller.edu; or Tak W. Mak: tmak@uhnresearch.ca

Abbreviations used in this paper: DP, dermal papilla; ERK, extracellular regulated kinase; ES, embryonic stem; IGF, insulin-like growth factor; IRS, inner root sheath; KO, knockout; MEK, MAPK/ERK kinase; ORS, outer root sheath; P, postnatal day; PGK, phosphoglycerate kinase; Phox, phagocyte oxidase; PI3K, phosphatidylinositol 3 kinase; Pten, phosphatase and tensin homologue on chromosome 10; RIPA, radioimmunoprecipitation assay; Sgk, serum and glucocorticoid responsive kinase; Tcf, T-cell factor; TOPgal, Tcf optimal promoter driving β-galactosidase; WT, wild type.

The Journal of Cell Biology, Vol. 170, No. 4, August 15, 2005 559–570
http://www.jcb.org/cgi/doi/10.1083/jcb.200504131

Holbro et al., 2003). The outcome of growth factor signaling is dependent on the cell type, the signal received, and the receptor. In the anagen hair follicle, multiple growth factors for tyrosine kinase receptors are present, including insulin-like growth factors (IGFs), EGF, FGFs, and PDGF (Stenn and Paus, 2001). Genetic analyses of these factors in mice have uncovered a surprising variety of hair defects ranging from the promotion of follicle morphogenesis (Liu et al., 1993) and differentiation of the hair shaft (Guo et al., 1996) to the induction of catagen (Sundberg et al., 1997) and maintenance of the supportive dermis (Karlsson et al., 1999). The two principle signaling routes that are activated by growth factor receptor tyrosine kinases are the Ras–Raf–MEK (MAPK/extracellular regulated kinase [ERK] kinase)–MAPK (Johnson and Lapadat, 2002) and phosphatidylinositol 3 kinase (PI3K)–PDK1–Akt pathways (Datta et al., 1999). *Akt1*-null mice exhibit retardation of postnatal hair follicle morphogenesis (Di-Poi et al., 2005), and mice that are double null for *Akt1* and *Akt2* die shortly after birth and exhibit pleotropic defects, including impaired skin and hair follicle development (Peng et al., 2003). However, the roles for these or other downstream pathway members in regulating the choice between proliferation and apoptosis in anagen hair follicles have remained elusive.

The serum and glucocorticoid responsive kinase (Sgk) family consists of three serine-threonine kinases that share a highly similar kinase domain with Akt family members, but their lack of a plasma membrane–targeting (pleckstrin homology) domain suggests possible nonoverlapping functions (for review see Lang and Cohen, 2001; Firestone et al., 2003). Sgk3 (also known as cytokine-independent cell survival kinase) is particularly interesting because it contains a Phox domain (first identified on phagocyte oxidase proteins), which prefers phosphatidylinositides that target the kinase to the early endosome rather than to the plasma membrane (Virbasius et al., 2001; Xu et al., 2001). Like conventional Akts, Sgk3 can be activated by IGF-1 and EGF in a manner that is dependent on tyrosine kinase receptor activation of PI3K (Kobayashi and Cohen, 1999; Kobayashi et al., 1999; Virbasius et al., 2001). Additionally, overexpression of Sgk3 protects against apoptosis in hematologic cells that have been deprived of IL-3 (Liu et al., 2000). On the basis of these findings, Sgk3 has been surmised to act as a cell survival kinase with properties similar to that of Akt.

Recently, it was reported that *Sgk3*-null mice display a hair coat defect, which was attributed to aberrations in Wnt signaling, altered proliferation, an absence of apoptosis, and a delayed onset of catagen (McCormick et al., 2004). Independently, we targeted *Sgk3* for ablation, but in analyzing the mice, we have come to a different conclusion as to the phenotypic consequences and underlying molecular basis of the defects involved. Although the loss of *Sgk3* results in reduced proliferation, it is actually accompanied not by delayed but rather by premature entry into catagen. Our studies reveal a requirement for Sgk3 in regulating the maintenance of the transit-amplifying matrix cell population that supplies the anagen bulb. By evaluating growth factor signaling in primary keratinocytes that were cultured from *Sgk3*-null mice, we discovered that keratinocytes lacking Sgk3 exhibit a paradoxically increased responsiveness to IGF-1, suggesting the existence of a novel feedback pathway in which Sgk3 acts to inhibit PI3K pathway activation. Our results provide the first documentation for a role of an Sgk/Akt kinase in governing the balance between the growing and destructive phases of the hair cycle.

Results

Mice lacking Sgk3 are viable and fertile

To determine the physiological role of Sgk3, we used homologous recombination in embryonic stem (ES) cells to generate *Sgk3* knockout (KO) mice. The targeting vector was designed to remove two critical exons of the Sgk3 kinase domain containing the catalytic core, including a lysine residue that is essential for ATP binding; stop codons were inserted just downstream of the exon 8 splice acceptor site (Fig. 1 A). Three independent clones (*Sgk3*-4, -17, and -44) carrying the mutated *Sgk3* allele were used for further analysis. F_1 heterozygotes originating from *Sgk3*-17 or -44 clones were intercrossed to produce homozygous F_2 progeny. Of 120 F_2 pups, 35 were +/+ (29%), 54 were +/− (45%), and 31 were −/− (26%), which is consistent with the expected Mendelian ratio. Southern blot hybridization of DNA from F_2 offspring demonstrated a presence of the targeted allele (Fig. 1 B). Northern blot analysis was consistent with a marked reduction of *Sgk3* transcripts in −/− skin (Fig. 1 C). Western blot analysis of lysates that were probed with an antibody against the Phox domain confirmed the presence of Sgk3 protein in keratinocytes that were cultured from the skins of newborn +/+ and +/− mice and confirmed the loss of Sgk3 protein in −/− mice (Fig. 1 D). Western analysis of skin fractions demonstrated that Sgk3 is present in the hair follicle fraction and is absent from the epidermal fraction at postnatal day (P) 5 (Fig. 1 E). This is consistent with the prior report that Sgk3 mRNA is expressed in the hair follicle root sheaths and matrix but not in interfollicular epidermis (McCormick et al., 2004). Western blot analysis detected Sgk3 protein throughout the synchronous progression of hair follicles from anagen through catagen and telogen (Fig. 1 E).

Mice lacking Sgk3 have an abnormal hair coat

Mice homozygous for the *Sgk3*-null allele (KO) were healthy and of normal size and weight. However, their whiskers and hair coats were distinctly abnormal (Fig. 2, A–M). Other epidermal-derived structures seemed normal; mammary gland function was intact, as KO females nursed pups to weaning without difficulty, sweat glands functioned properly as determined by an iodine sweat test (unpublished data), sebaceous glands produced sebum as determined by an oil red O stain of postnatal and adult back skin (unpublished data), and teeth appeared fully functional.

Newborn *Sgk3*-null pups were identifiable by their whiskers, which bent erratically and often pointed forward or outward, lacking the organized straightness of normal whisker sets (Fig. 2, G and H). Throughout life, their hair coat was sparse and their epidermis was visible through the coat (Fig. 2, A–D). The hair shafts themselves were malformed. In contrast to the normal

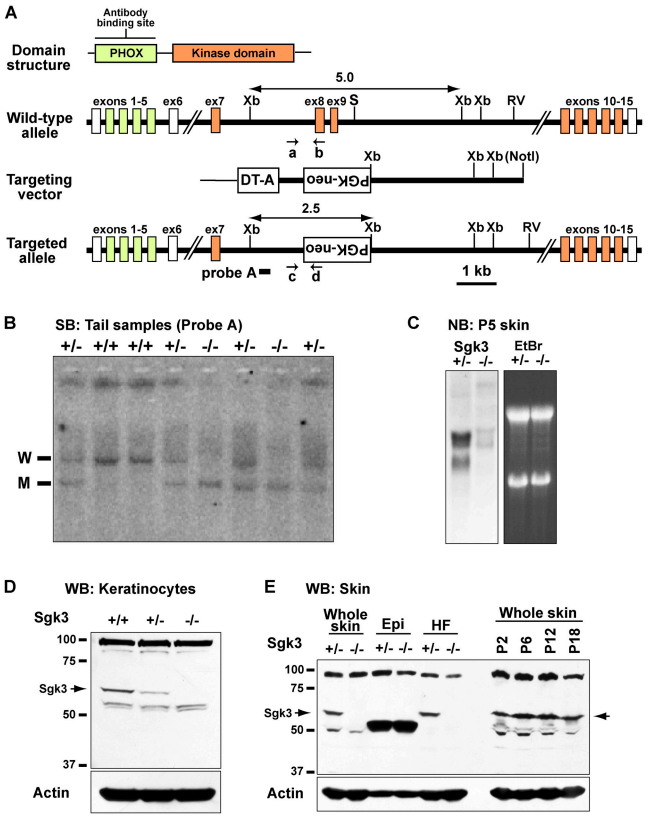

Figure 1. **Targeting of the Sgk3 gene by homologous recombination.** (A) Schematic of WT mouse Sgk3 domain structure, gene locus, targeting construct, and mutated Sgk3 allele. Exons 8 and 9 were replaced with PGKneo, and diphtheria toxin A was used for negative selection. Indicated are the antibody binding site, the 5′ external probe A that was used for Southern hybridization, predicted sizes of hybridizing fragments, and primer pairs that were used for PCR. Short arrows represent the primers that were used for PCR analysis of WT (a and b) or mutant (c and d) alleles. RV, EcoRV; Xb, XbaI; S, SmaI. (B) Southern hybridization analysis (SB) of F2 offspring of intercrosses of Sgk3 mutant F1 mice. Tail genomic DNA digested with XbaI was probed with external probe A; W, WT allele; M, mutant allele. (C) Northern analysis (NB) of Sgk3 mRNA expression in total mRNA extracted from P5 skin. EtBr, ethidium bromide. (D) Western immunoblot (WB) shows the presence of Sgk3 in cultured keratinocytes. (E) Immunoblot of dispase-separated epidermis and dermis hair follicle (HF) fractions shows Sgk3 (arrows) in the hair follicle fraction but not in the interfollicular epidermal fraction and also demonstrates that Sgk3 is expressed throughout the hair cycle in whole skin. Extra bands on Western blots are a result of nonspecific signal. Actin, loading control.

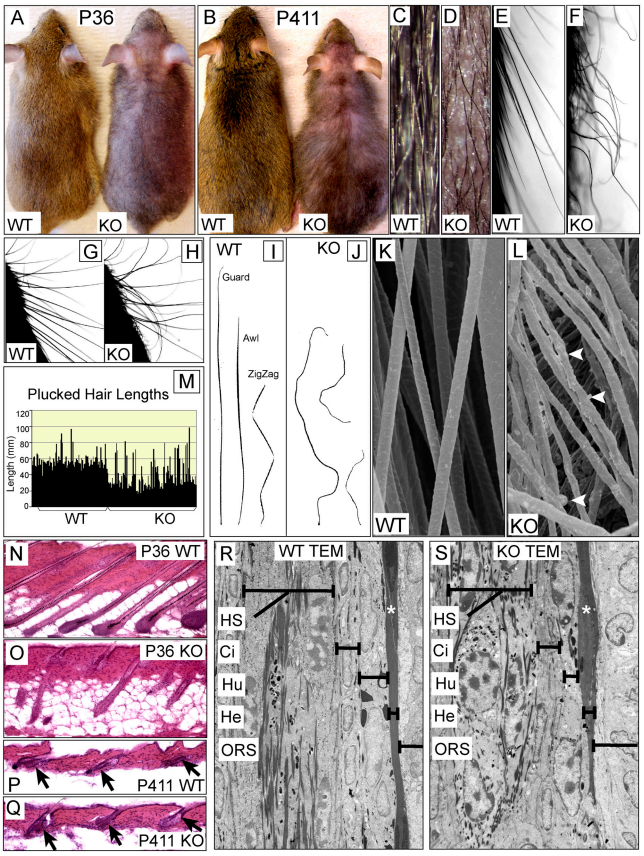

Figure 2. **Sgk3 is required for normal hair coat production.** Adult mice (P36 and P411) have a sparse, uneven hair coat (A–D) and irregular hair shafts when seen in profile (E and F). Whiskers are malformed (G and H). Plucked hairs (I and J) lack normal guard, awl, or zigzag hairs. Scanning EM (K and L) shows KO hairs to be irregular and thin with occasional malformed cuticles (arrowheads). Sgk3-null plucked hairs are shorter than WT hairs, with the exception of guard hairs (M). Histology of adult back skin demonstrates that a sparse coat is not caused by the loss of hair follicles (arrows; N–Q). Transmission EM (TEM) of P3 follicles verifies the presence of all cell types in KO follicles (R and S), including the three layers of the IRS. Note the normal keratinization of Henley's layer of the IRS in the upper bulb (asterisks). HS, hair shaft; Ci, IRS cuticle; Hu, Huxley's layer of the IRS; He, Henley's layer of the IRS; ORS, outer root sheath.

coat, which consists of straight (guards and awls) and kinked hairs (zigzags), *Sgk3*-null hairs lacked straight segments or organized kinks and, instead, curled and bent randomly (Fig. 2, E, F, I, and J). Scanning EM revealed that *Sgk3*-null hairs were atypically thin, displaying thickened knobby regions and thin spindly regions (Fig. 2, K and L). The cuticle cells that provide a shingle-like surface to the hair shaft were present in KO hairs, although they were often poorly adherent to the shaft. Quantitative analysis revealed that the majority of KO hairs were unusually short, with the exception of guard hairs, which constitute a relatively minor portion of the overall hair coat (Fig. 2 M). Histological analyses of P36 and P411 skins showed no difference in overall follicle density (Fig. 2, N–Q, arrows). Transmission EM indicated that all the morphologically distinct cell types were present in KO follicles, including the three IRS layers; keratinization of Henley's layer in the upper bulb occurred normally (Fig. 2, R and S). However, alterations in the shape and size of cells within the hair shaft and IRS were evident in KO follicles. It was difficult to find good examples of medullated hair shafts in the KO. Altogether, these data indicated that the sparsity seen in the KO hair coat is rooted in structural abnormalities within the hairs rather than in a reduction in follicle numbers.

Development and differentiation of hair follicles does not require Sgk3

To determine whether the loss of Sgk3 compromised hair follicle morphogenesis or differentiation, we first conducted a histological analysis of postnatal skin. Through P2, the morphology and biochemistry of KO hair follicles were indistinguishable from wild type (WT) by histology and immunofluorescence microscopy with markers that typified differentiation of the hair shaft (AE13; stains hair keratins), IRS (AE15; stains trichohyalin granules), and companion cell layer (K6; Fig. 3, A–H).

A previous study on an independently generated *Sgk3*-null mouse attributed aberrations in the postnatal *Sgk3*-null hair coat to a loss of precortical Wnt signaling (McCormick et al., 2004). Wnt signaling is required for hair keratin gene expression (van Genderen et al., 1994; Zhou et al., 1995; DasGupta and Fuchs, 1999), and the normal hair keratin levels that are found in P2 *Sgk3*-null follicles seemed inconsistent with impairment of this pathway. To resolve this discrepancy, we mated *Sgk3*-null mice to a Wnt reporter mouse that expressed β-galactosidase under control of the T-cell factor (Tcf)/lymphoid enhancer factor (Lef) optimal promoter, which contained multimerized Lef1/Tcf-binding sites (Tcf optimal promoter driving β-galactosidase [TOPgal]; DasGupta and Fuchs, 1999). We determined canonical Wnt activity by using two separate methods: in situ enzymatic detection of the β-galactosidase substrate and immunoblot of whole skin for total β-galactosidase protein.

Both WT and KO P2 follicles displayed strong transgene expression in the precortical cells that express the natural Wnt target genes encoding hair keratins (Fig. 3, I and J). Even at P6, when follicles were in full anagen, TOPgal activity was prominent and of similar intensity in WT and KO follicles (Fig. 3, K and L). Immunoblot analysis also revealed comparable levels of TOPgal reporter expression (Fig. 3 M). Altogether, these findings argue against an essential role for Sgk3 either in governing hair follicle differentiation or in permitting Wnt signaling.

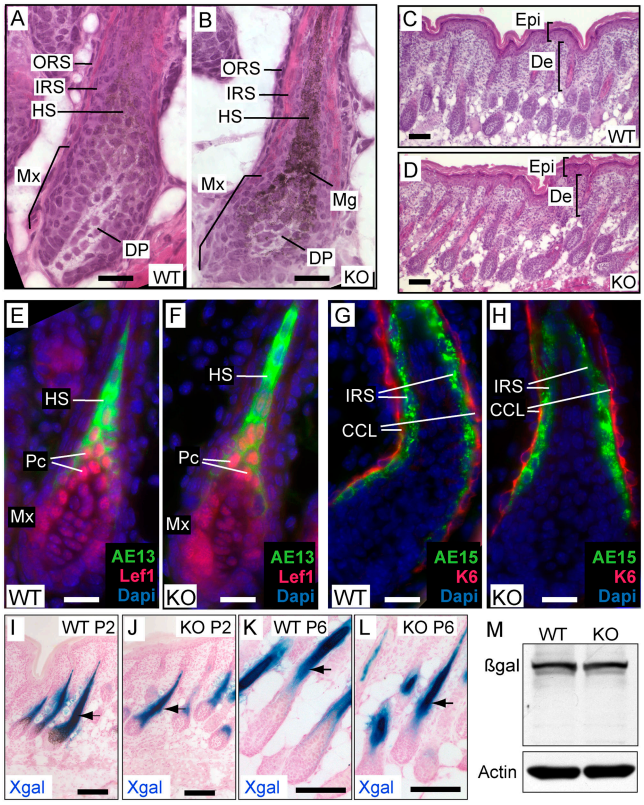

Figure 3. **Hair follicle morphogenesis is normal in Sgk3-null mice until P2.** At P2, follicles have normal histology by hematoxylin and eosin (A and B), including ORS, IRS, and hair shaft (HS) layers. Follicle number and density is normal (C and D). Differentiation markers AE13 (hair keratins; hair shaft cortex), AE15 (trichohyalin; IRS), and keratin 6 (K6; companion cell layer [CCL]) are normal in KO follicles at P2 (E–H). Wnt pathway member Lef1 (lymphoid enhancer factor 1) is normal (E and F); mating Sgk3-null mice to Wnt reporter TOPgal mice reveals normal intensity of reporter activity in KO hair follicles at P2 and P6 (I–L). Arrows represent blue Xgal precipitate, demonstrating activity of the TOPgal Wnt reporter. Immunoblot of whole skin lysates at P2 confirms equal amounts of β-galactosidase (M). Mx, matrix; DP, dermal papilla; Epi, epidermis; De, dermis; Pc, precortex; Mg, melanin granules. DAPI, nuclear counterstain; Xgal, β-galactosidase enzymatic substrate. Bars (A, B, and E–H), 20 μM; (C, D, and I–L) 100 μM.

Sgk3-null follicles show abnormal anagen morphology and fewer bulb cells

In the course of our Wnt-signaling studies, we observed morphological differences in P6 follicles that were not detected in P2 skin. Most notably, follicles lacking Sgk3 seemed to have arrested in early anagen. Closer inspection revealed that as early as P3, *Sgk3*-deficient hair follicles diverged from WT follicles. In contrast to normal follicles, which were still growing downward into the subcutis between P3 and P6, KO hair bulbs arrested midway between the epidermis and the base of the subcutis (Fig. 4, A–D). Closer inspection revealed a distinctly smaller hair bulb; rather than elongating to form the typical robust structure of the normal P6 anagen phase bulb, KO P6 bulbs remained the size of P2 bulbs (Fig. 4, E–H). Similarly, the associated DPs, which were marked by alkaline phosphatase expression, remained small and round rather than becoming long and thin, as is typical of WT P6 DPs (Fig. 4, E–H). These defects were not merely a developmental delay in anagen. Rather, *Sgk3* KO hair follicles never attained a normal mature anagen matrix.

We counted the number of epithelial nuclei that were visible per follicle within 10-μM sagittal skin sections. At P2, when bulb sizes were approximately the same, the number of matrix cells from the bottom of the bulb to the top of the DP was similar between WT and KO follicles (Fig. 4 I). Between P2 and P6, however, the matrix cell population increased dramatically in WT follicles, but hardly changed in KO follicles. These data verified that the lack of expansion in the bulb size of *Sgk3*-null hair follicles was reflected in a corresponding failure to expand the matrix population.

Reduced proliferation and mildly increased apoptosis accounts for reduced cell number in Sgk3-null bulbs

A priori, a reduction in bulb cell number could be a result of an increase in the rate at which cells are lost from the bulb, either through cell death or differentiation. Alternatively, it could be a resut of a decrease in the rate at which cells are gained in the bulb through proliferation or migration from the outer root sheath (ORS). To distinguish between these possibilities, we evaluated rates of apoptosis and proliferation at P2 and P6.

Because Sgk3 was initially identified as a survival kinase (Liu et al., 2000), one explanation for the reduced cell number could be increased sensitivity to proapoptotic signals. Analysis of apoptosis by activated caspase 3 detection in tissue sections (see Fig. 6) and confirmed morphologically by transmission EM (Fig. 4, J and K) revealed an increase in the number of apoptotic cells in KO P6 follicles. However, even though apoptosis was more frequent in *Sgk3*-null follicles than in their WT counterparts, many KO follicles had no apoptotic cells, and the

overall number of cells undergoing apoptosis was quantitatively too low to explain the large reduction in bulb cell number that was evident at P6 (Fig. 4 I).

Next, we measured proliferation in WT and *Sgk3*-null hair bulbs. After administering a 2-h pulse of BrdU, we quantified the number of labeled cells (Fig. 4, L–O). At P2, the number of S phase cells in the bulbs were similar, which is consistent with the equivalent histology and cell number. By P6, however, the number of proliferating cells in WT bulbs had increased, whereas KO bulbs displayed fewer proliferating cells than at P2. This difference resulted in a substantially reduced number of dividing cells in KO bulbs at P6 when compared with WT, which is on par with the decline in overall bulb cell number (Fig. 4 I). The number of BrdU-positive cells in the ORS was slightly reduced in P6 KO follicles, although the measurement did not reach significance (unpublished data). Based on these findings, the difference in bulb cell number appears to be largely attributable to a reduction in proliferation with a small contribution from increased apoptotic death.

Fate mapping S phase cells suggests that the bulb defect results from inadequate recruitment or regeneration of progenitor cells

Fewer dividing cells in *Sgk3*-null bulbs could result from either slower progression through the cell cycle, a reduced number of divisions before cell cycle exit, or a reduced supply of bulb progenitor cells (Fig. 5 B). Slower progression through the cell cycle would result in a bulb with equal or reduced cell number and with a reduced rate of production of differentiated hair shaft layers. On the other hand, premature exit from the cell cycle, which is possibly associated with premature differentiation, could explain the lower proliferation and also the reduced cell number. To evaluate the rate of cell cycle exit and entry into differentiation pathways, we pulsed pups with BrdU for 4 h and then chased for 12 or 20 h to monitor the fates of dividing cells (Fig. 5 A). The cell cycle in the anagen matrix is known to be ~18 h (Lehrer et al., 1998). By costaining for BrdU and differentiation markers of the hair shaft, we measured the number of dividing cells that progress to terminally differentiate versus the number that remain in the lower germinative region of the matrix. The data are compiled in Fig. 5 D.

The number of BrdU-positive matrix cells that progressed to terminally differentiate was markedly reduced in the KO. However, the total number of matrix cells was also reduced concomitantly, and, hence, the percentage of BrdU-labeled cells that differentiated was comparable with the WT and *Sgk3* mutant bulbs (Fig. 5, C and D). Because the number of differentiated matrix cells did not increase in KO bulbs, the anagen bulb defect could not be explained by premature exit from the cell cycle with premature differentiation. As KO bulbs showed no signs of accumulating undifferentiated cells between the BrdU-positive germinative region and the differentiating compartment (Fig. 5, C and D), early cell cycle exit without premature differentiation also did not appear to be causative. Finally, because the reduced bulb proliferative number was proportional to the reduced bulb cell number, the percentage of bulb cells

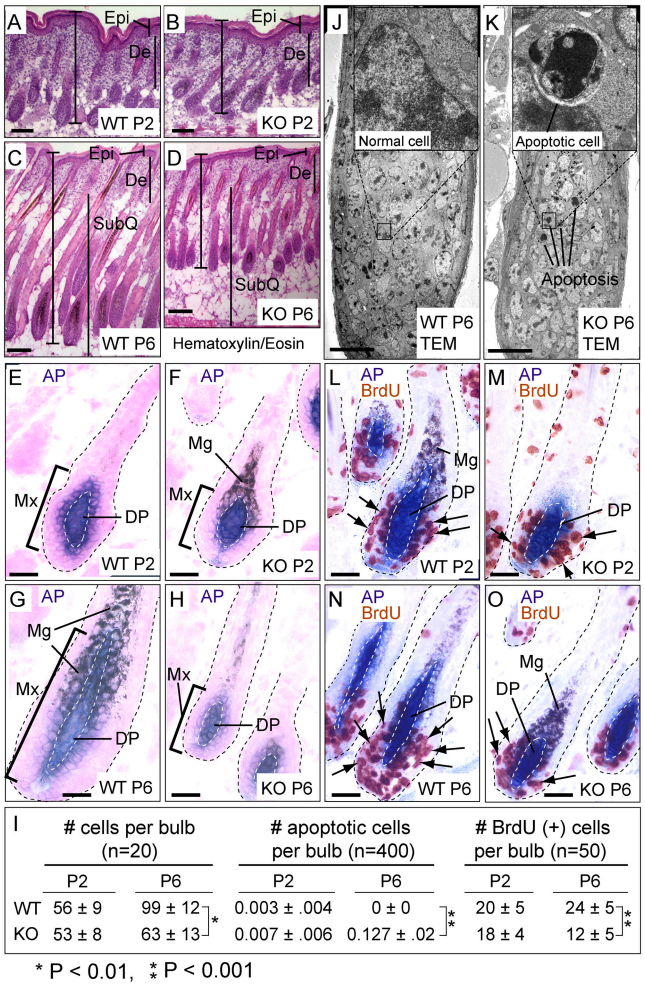

Figure 4. **Anagen maturation is impaired in Sgk3-null hair follicles.** Histology is similar at P2 (A and B) but by P6, Sgk3-null follicles are smaller and fail to grow down to the bottom of the subcutis (C and D). At P6, the shortened KO bulb has a smaller, rounded DP relative to the long, thin DP of WT follicles (G and H). Apoptotic cells are seen in some KO follicle bulbs (J and K); although many P6 bulbs show no apoptotic cells, some have as many as six. Incorporation of BrdU in KO bulbs at P6 is reduced relative to WT bulbs (L–O). Arrows represent examples of BrdU-positive nuclei. (I) Quantification shows that total cell number is reduced in KO bulbs at P6, apoptotic cell number is increased, and proliferation is markedly decreased. Epi, epidermis; De, dermis; SubQ, subcutis; Mx, matrix; Mg, melanin granules; TEM, transmission EM; AP, alkaline phosphatase. Bars (A–D), 100 μM; (E–H and L–O) 20 μM; (J and K) 10 μM.

that were proliferative was unchanged (Fig. 5 D), suggesting that slowed cell cycle does not cause the defect. Altogether, these experiments indicate that reduction in the matrix cell pool in *Sgk3*-null follicles results from reduced recruitment or self renewal of progenitor cells of the matrix and not from impaired proliferation of the matrix cells themselves.

Sgk3-null hair follicles enter catagen earlier rather than later

One theory regarding the transition from anagen to catagen is that the bulb exhausts its supply of transiently amplifying matrix cells. If this model is correct, our findings would predict that the *Sgk3*-null mouse should enter catagen early. To test this hypothesis, we analyzed the kinetics and biochemistry of

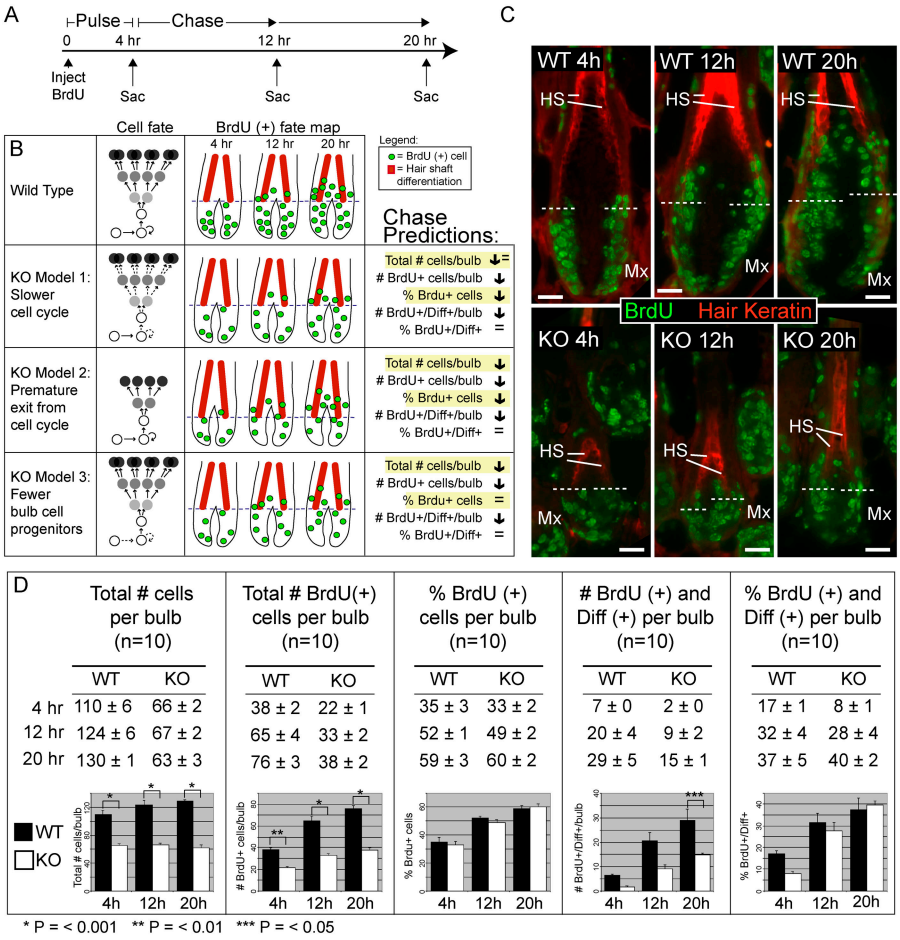

Figure 5. **BrdU fate mapping distinguishes between models for reduced bulb cell number and proliferation.** (A) Experimental design; mice pulsed with BrdU at P4 were chased for 12 or 20 h. (B) Predicted outcomes for three models. The percentage of Brdu+ cells reflects the percentage of total bulb cells that are BrdU+. The No. of BrdU+/Diff+/bulb reflects the cells per bulb that are positive for BrdU and are above the boundary (dotted lines) of differentiation marker expression. The percentage pf BrdU+/Diff+ is the percentage of BrdU+ cells that are above the boundary relative to the total. Distinguishing between an intrinsic proliferative defect in matrix cells (models 1 and 2) and a defect in the recruitment or regeneration of matrix cells (model 3) relies on the measurement of the percentage of BrdU+ cells. (C) Representative sections demonstrate movement of BrdU-labeled cells. Note that the total number of BrdU-positive cells at 20 h is double the number at 4 h, which is consistent with the expected division after S phase. This confirms that ongoing labeling beyond 4 h does not occur. Dotted lines mark the lower limit of hair keratin expression. HS, hair shaft; Mx, matrix. Bars, 20 μm. (D) Quantification reveals that the most likely explanation for reduced cell number is impaired recruitment or regeneration of progenitors. Error bars represent SEM.

this critical stage of the hair cycle in *Sgk3*-null mice and their WT counterparts. The results are compiled in Fig. 6.

In WT mice, the first anagen lasted from approximately P2 through P14, and by P15, follicles had synchronously entered catagen (Fig. 6, A–E). Although some variability is known to exist among different mouse strains, our data were in good agreement with previously reported analyses of normal mice (Muller-Rover et al., 2001). In striking contrast, *Sgk3*-null follicles displayed a catagen-like morphology as early as P9, and by P12, most follicles were regressing (Fig. 6, F–H). Remarkably, by P12, follicles in the upper back had already completed catagen and telogen and had actually reentered anagen (Fig. 6, EE). By P15, most *Sgk3*-null follicles had already initiated the next hair cycle (Fig. 6 I). Reentry into anagen did not begin in WT littermates before P20 (not depicted). In P18 KO skin, histological signs of anagen were seen in some follicles and catagen was seen in others, indicating a similar rapid transition from anagen to catagen in the second hair cycle (Fig. 6 J).

Although the hair cycle phases are associated with histological differences, transitions from one hair cycle stage to another are best evaluated by a combination of biochemistry and histology. To unequivocally establish early entry into catagen and to determine whether the anagen to catagen transition is biochemically normal in *Sgk3*-null follicles, we determined endogenous alkaline phosphatase activity of DP cells (Muller-Rover et al., 2001) and BrdU incorporation of matrix cells throughout the hair cycle. This combinatorial method enabled us to precisely track the hair cycle stages from P6 through P18.

Normal anagen is marked by robust BrdU incorporation in the matrix and by characteristic DP morphology (Fig. 6, K–N); during catagen, BrdU incorporation declines, and the DP becomes a round, small cluster of cells (Fig. 6 O). In *Sgk3*-null follicles, a dramatic reduction in BrdU incorporation in the matrix with the characteristic catagen evolution of the DP confirmed that catagen was well underway by P9 (Fig. 6, P and Q). Interestingly, despite premature onset, the morphology and biochemistry of catagen appeared to be normal. Kinetics of the transition through catagen into the first telogen and the following anagen also seemed to be largely normal, proceeding over a period of ~6 d (Fig. 6, compare M–O with P–R).

We also addressed whether the absence of Sgk3 altered the rate of apoptosis during the hair cycle. A sensitive and reliable method to capture this rapidly occurring process in hair follicles is immunofluorescence microscopy with antibodies against activated caspase 3, which is a specific and direct consequence of apoptotic machinery activation. Representative frames of these data are shown in Fig. 6 (U–DD). Normal follicles only exhibited anticaspase 3–labeled cells as they entered catagen, when a burst of caspase 3 activity was detected in the bulb and epithelial strand as it regressed upward. In *Sgk3*-null follicles, anticaspase 3 labeling was also restricted largely to these sites and stages in

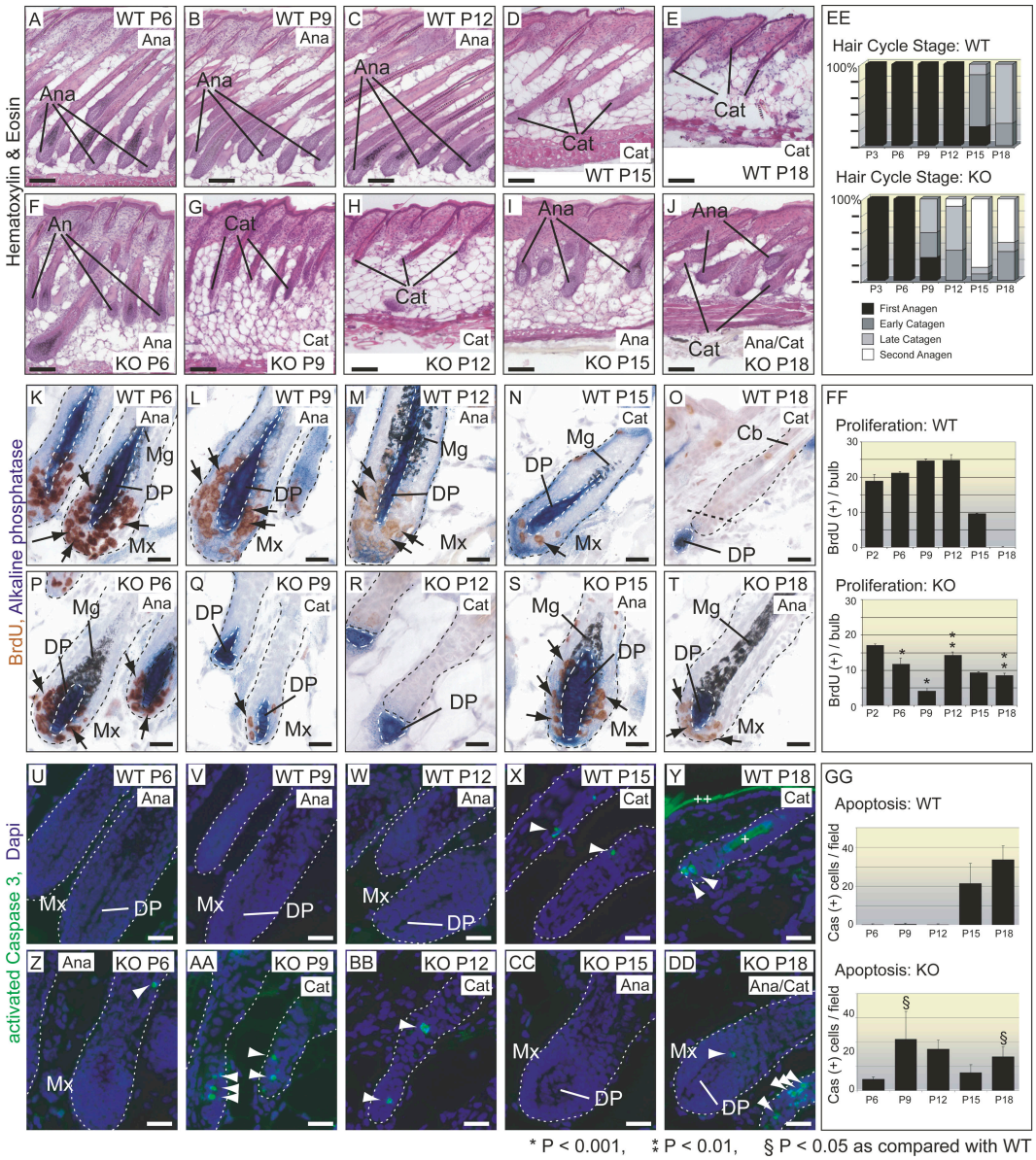

Figure 6. **Hair follicles lacking Sgk3 enter catagen prematurely.** Histology shows the onset of catagen in WT skin at P15 and in KO skin at P9 (A–J). (EE) Quantification of hair cycle stage based on DP morphology that was visualized by alkaline phosphatase (Muller-Rover et al., 2001). Anagen (all stages); early catagen (catagen I–III); late catagen (IV–VIII). Note that Sgk3-null follicles enter catagen prematurely; by P15, they have entered the second anagen. (K–T) BrdU staining and DP morphology suggest that KO catagen traverses normal stages. Arrows represent BrdU-positive nuclei. (O) Straight dotted line demarcates the bottom of the permanent portion of the hair follicle. (FF) Quantification of BrdU incorporation confirms the appropriate decline in proliferation as KO follicles enter catagen. (U–DD) Staining for activated caspase 3 shows that apoptosis in Sgk3-null follicles increases normally during catagen, excluding massive apoptosis as a mechanism to explain reduced bulb cell number or premature catagen. (Y) Plus signs indicate autofluorescence of the hair shaft (+) and differentiated epidermis (++). Arrowheads, caspase (+) cells. (GG) Quantification of apoptosis confirms the increased number of apoptotic cells in KO skin. Mx, matrix; Ana, anagen; Cat, catagen; Mg, melanin granules; DP, dermal papilla; Cb, Club hair. Error bars represent SEM. Bars (A–J), 100 μM; (K–DD) 20 μM.

the hair cycle (Fig. 6 DD). We did see occasional apoptotic cells in KO anagen bulbs, but, as a result of the absence of morphological criteria to distinguish anagen VI from catagen I, we cannot exclude the possibility that these events represent very early catagen. The differences that were seen in the timing at which anticaspase 3 labeling was detected correlated well with the premature entry of *Sgk3*-null follicles into catagen. Additionally, the mixture of anagen and catagen phase follicles that was noted previously in P18 *Sgk3*-null skin was further confirmed by anticaspase 3 staining (Fig. 6 DD). Although unprecedented for such an early age, this asynchrony in cycling of the *Sgk3*-null hair coat could reflect the progressive asynchrony that normally occurs with successive hair cycles in WT mice.

Fig. 6 (EE–GG) provides quantification of all of the data from the experiments that are illustrated in Fig. 6. These data graphically illustrate the defect in *Sgk3*-null follicles as a markedly shortened anagen phase of the hair cycle. Altogether, our data suggest that in the absence of Sgk3, reduced maintenance or supply of matrix progenitor cells results in impaired maturation of anagen followed by precocious entry into catagen.

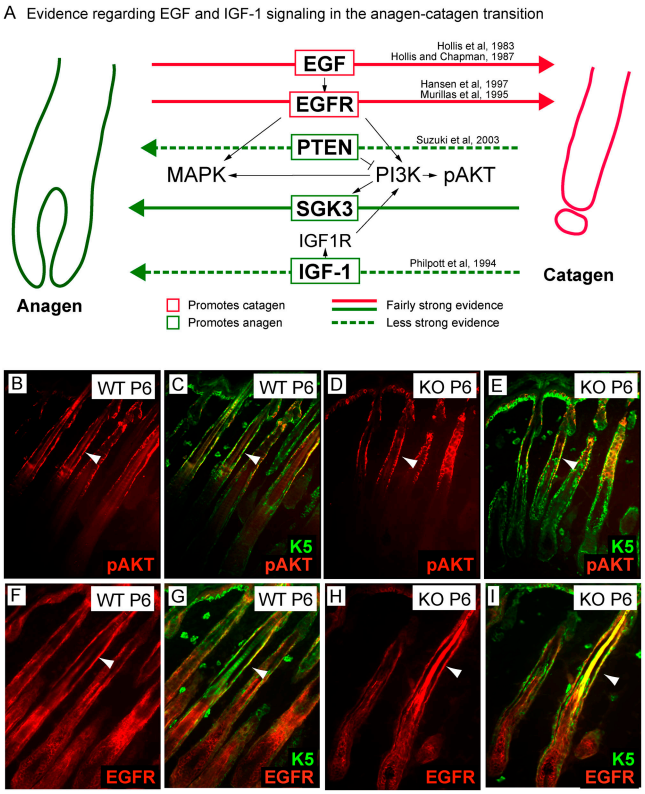

Figure 7. **Growth factor signaling elements are present in the hair follicle.** (A) Schematic depicting EGF and IGF-1 pathways and known effects on the anagen to catagen transition. Note the strong evidence that EGF and EGFR promote catagen, which are consistent with the observation that Pten, which is inhibitory to PI3K, may promote anagen. (B–I) Localization of growth factor signaling in the hair follicle. Phospho-Akt is present strongly in the upper ORS, colocalizing with K5, in both WT and KO skin at P6 (B–E). EGFR is expressed in the ORS, colocalizing with K5, and in the interfollicular epidermis and hair bulb (F–I). Arrowheads indicate colocalization with K5 in the ORS.

Sgk3-null keratinocytes display increased downstream growth factor signaling in response to IGF-1

Several tyrosine kinase receptor growth factors have been implicated in the anagen–catagen transition, including EGF, IGF-1, and FGF5 (Fig. 7 A; Philpott et al., 1994; Murillas et al., 1995; Hansen et al., 1997; Sundberg et al., 1997). Interestingly, the morphological and hair cycle defects that were observed in *Sgk3*-null follicles were similar to those described upon injection of EGF into mice and sheep (Moore et al., 1981, 1982; Hollis et al., 1983; Hollis and Chapman, 1987).

To evaluate where downstream growth factor signaling occurs in the hair follicle, we performed immunofluorescence for phosphorylated (i.e., active) forms of ERK 1/2 and Akt. The phospho-ERK antibody revealed specific staining at P6 in the interfollicular epidermis without clear localization in the hair follicle (unpublished data). However, immunofluorescence for phospho-Akt revealed specific staining in K5-positive cells that were located in the upper ORS (infundibulum) above the stem cell compartment and in the ORS below the stem cell compartment (Fig. 7, B–E). Throughout the hair cycle, phospho-Akt patterns were similar from early anagen (P2) through late catagen (P18) without significant alteration in distribution or intensity (unpublished data). As previously noted (Hansen et al., 1997), anti-EGF receptor (R) immunofluorescence showed labeling in the ORS, interfollicular epidermis, and matrix (Fig. 7, F–I); this staining persisted into catagen (unpublished data). Intriguingly, EGFR and phospho-Akt labeling were present in a region of the anagen and catagen phase ORS where matrix cell progenitors are thought to reside (Taylor et al., 2000; Oshima et al., 2001). Based on these data and the observation that the Sgk3 loss-of-function phenotype resembles EGF gain-of-function results, we wondered whether Sgk3 might modulate downstream growth factor signaling.

To test this possibility, we took advantage of the ability to culture primary keratinocytes from newborn mouse skin (i.e., at an age that preceded the defects seen in *Sgk3*-null animals). We determined the response of WT and KO keratinocytes to two key growth factors, EGF and IGF-1, by measuring the activation of two principle downstream pathways, Ras–Raf–MEK–MAPK (ERK 1/2) and PI3K–PDK1–Akt.

Within minutes after EGF addition, both WT and KO keratinocytes displayed a rapid increase in activated (phosphorylated) ERK 1/2 (Fig. 8 A). This response appeared to be comparable in magnitude and kinetics irrespective of the status of Sgk3. The kinetics and levels of Akt activation after EGF addition were also comparable in WT and KO cells (Fig. 8 A). Thus, the loss of Sgk3 in keratinocytes did not appear to influence EGF-mediated activation of either the MAPK or Akt pathways.

Surprisingly, when the experiments were repeated using IGF-1 rather than EGF, the outcomes were different, as the results were dependent on the presence of Sgk3. In the absence of Sgk3, both MAPK and Akt were activated to higher levels than in WT keratinocytes (Fig. 8 B). Antibodies to total ERK 1/2 and Akt showed that these differences were not caused by changes in the overall levels of ERK 1/2 or Akt proteins but rather were selective for the phosphorylated forms (Fig. 8 B). These data suggest that Sgk3 reduces the downstream response of keratinocytes to IGF-1.

The molecular brake exerted by Sgk3 appeared to be one that impacted equivalently on both arms of the signaling pathway. A priori, this could be a reflection of an effect on a shared member of these corridors, such as the tyrosine kinase receptor itself. However, we noticed that the kinetics of ERK 1/2 activation by IGF-1 were delayed relative not only to Akt activation but also to EGF-mediated activation of ERK 1/2 (Fig. 8, A and B). This observation led us to wonder whether ERK 1/2 and Akt activation by IGF-1 might be in a linear pathway, which would place them both downstream of PI3K in primary keratinocytes.

To test this possibility, we pretreated keratinocytes with a PI3K-specific dose of wortmannin and stimulated with IGF-1 or EGF. As shown in Fig. 8 C, wortmannin effectively eliminated the IGF-1 activation of ERK 1/2 but had no effect on EGF activation of ERK 1/2. As expected, wortmannin blocked Akt activation in both WT and KO keratinocytes in response to both IGF-1 and EGF (Fig. 8 C). These findings demonstrate that the ability of IGF-1 to stimulate ERK 1/2 activation is dependent on PI3K activity in primary keratinocytes. Also,

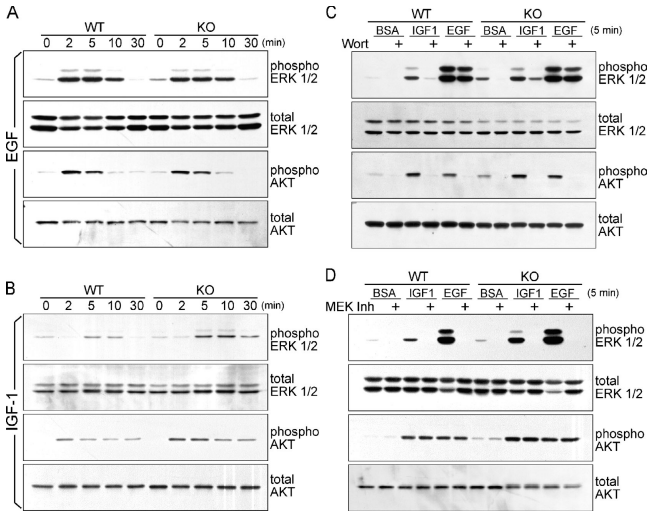

Figure 8. **Growth factor signaling is abnormal in Sgk3-null keratinocytes.** (A) Treating WT and KO primary keratinocytes with 10 ng/ml EGF reveals normal kinetics of the activation of ERK 1/2 and Akt. (B) In response to 50 ng/ml IGF-1, Sgk3-null keratinocytes exhibit increased activation of ERK 1/2 and Akt. (C) In primary keratinocytes, IGF-1–mediated activation of ERK 1/2 is dependent on PI3K activation, whereas EGF-mediated ERK activation proceeds independently of PI3K. Cells were pretreated with 100 nM wortmannin for 30 min before stimulation. (D) PI3K-dependent IGF-1 activation of ERK does not indicate codependence of PI3K and ERK pathways; phosphorylation of Akt is unaffected by treatment with MEK inhibitor 444937. Cells were pretreated with 1 μM 444937 for 30 min before stimulation. Antibodies are against phosphorylated (activated) or total ERK 1/2 or AKT 1–3 proteins.

enhanced ERK 1/2 and Akt activation after IGF-1 may both result from increased PI3K signaling in *Sgk3*-null keratinocytes.

Finally, it was important to determine whether PI3K dependence on ERK 1/2 activation by IGF-1 resulted from an interdependence of the MAPK and PI3K pathways or, alternatively, resulted from unidirectional activation of MAPK through PI3K. To distinguish between these two possibilities, we pretreated keratinocytes with the specific MEK inhibitor 444937 and assayed for activation of ERK 1/2 and Akt. In all cases, ERK 1/2 activation was quantitatively blocked by MEK inhibition, which did not impair Akt activation (Fig. 7 D). These data demonstrate that ERK 1/2 activation is dependent on both the MEK kinase and PI3K in response to IGF-1 in keratinocytes but that Akt activation is independent of MEK activation.

Discussion

Our findings uncover a novel role for a member of the Akt/Sgk family of serine-threonine kinases in maintaining the pool of hair progenitor cells and in regulating the transition from life to death at the end of the growth phase of the hair cycle. We discovered that the loss of function of Sgk3 reduces the supply of transit-amplifying progenitor cells and causes premature entry into the apoptotic regression phase of the hair cycle. Finally, we placed Sgk3 within the framework of tyrosine kinase growth factor receptor signaling, discovering a unique ability of Sgk3 to temper the effects of IGF-1–induced PI3K signaling.

Tyrosine kinase receptor activation and the anagen to catagen transition

The relation between growth factor signaling and the anagen–catagen transition has remained poorly understood for decades. Mice lacking FGF5 enter catagen late, suggesting an important role for FGF receptor signaling in the regulation of this transition (Hebert et al., 1994; Sundberg et al., 1997). This said, it has been suggested that FGF5, which is expressed in the ORS, may act on DP cells (Rosenquist and Martin, 1996), providing the potential for this interesting factor to regulate catagen through mesenchymal–epithelial interactions.

In the early 1980s, experiments showed that EGF promotes early transition from anagen to catagen, which is associated with decreased proliferation and increased apoptosis (Hollis et al., 1983; Hollis and Chapman, 1987). Genetic loss of function of the EGF receptor in mice causes premature differentiation in the hair bulb along with delayed catagen (Murillas et al., 1995; Hansen et al., 1997). Because excessive EGF signaling promotes catagen and the loss of EGFR promotes premature differentiation, it seems that the dose of EGF signaling in normal anagen is carefully balanced, supporting the relevance of downstream regulators that modulate pathway strength.

IGF-1 has also been implicated in hair cycle regulation, although the evidence is less strong than for EGF. It is curious that in keratinocytes, we see a difference with IGF-1 treatment but not with EGF treatment; this may be related to contextual differences in cultured keratinocytes as compared with growth factor responsive cells in living skin. IGF-1 is expressed by the DP, and IGF-1R is found in the matrix (for review see Su et al., 1999a). Genetic models of IGF-1 function in skin include transgenic mice overexpressing IGF-1 (Bol et al., 1997; Su et al., 1999b; Wilker et al., 1999; DiGiovanni et al., 2000) as well as the IGF-1R KO (Liu et al., 1993), but the hair cycle has not been evaluated in any of these animals. Human hair follicles in organ culture are reported to enter a catagen-like state upon withdrawal of IGF-1 from the culture medium (Philpott et al., 1994). It is possible that IGF-1 produced by the DP might signal to adjacent matrix cells expressing IGF-1R, regulating the choice between proliferation, differentiation, and apoptosis.

Downstream events of receptor activation and the anagen to catagen transition

Downstream of the growth factor ligand, less is understood about receptor tyrosine kinase signaling in the anagen to catagen transition. Our findings predict a role for PI3K in the onset of catagen. Consistent with this idea, skin epithelium lacking the PI3K inhibitor phosphatase and tensin homologue on chromosome 10 (Pten) shows decreased skin thickness at P10, and it has been suggested that follicles might enter catagen early (Suzuki et al., 2003). Because loss of Pten should result in excessive activation of PI3K (Sulis and Parsons, 2003), early catagen in follicles lacking Pten is consistent with PI3K exerting procatagen effects.

Akt1 and *Akt2* double KO mice have delayed hair follicle development, but the hair cycle was not evaluated (Peng et al., 2003). Our findings that *Sgk3* KO mice have a hair cycle defect in the presence of Akt1 and Akt2 suggest that even if these Akts

function in regulating the hair cycle, their effects are likely to be distinct from those of Sgk3. The presence of activated PI3K in the ORS, combined with our findings of increased PI3K signaling in Sgk3-null keratinocytes and an inadequate supply of matrix precursors in KO follicles, raises the interesting, unanswered questions of whether ORS progeny supply cells to the bulb and, if so, whether PI3K might regulate this process.

Our studies in culture reveal that in the absence of Sgk3, IGF-1 signaling through PI3K is more active, implying that Sgk3 causes feedback inhibition on PI3K signaling in keratinocytes. Because Sgk3 contains a Phox domain, which targets it to the early endosome, Sgk3 might modulate tyrosine kinase receptor signaling complexes as they are activated and internalized from the plasma membrane. Recent studies in other cell types have shown that Phox domain targeting to the early endosome is required for Sgk3 activation by both IGF-1 and EGF (Virbasius et al., 2001; Xu et al., 2001). Furthermore, endosomes containing Sgk3 colabel with internalized EGF at 5 and 15 min after cells are treated with labeled EGF (Xu et al., 2001).

Finally, the role of Sgk3 in maintaining matrix progenitors may not be its only role in the hair follicle given the poor coat quality. Because proliferation is required to produce hair shaft and IRS layers, reduced proliferation and early termination of the growth phase can readily explain the reduced hair shaft diameter and length. However, disorganization of the differentiating layers, although possibly a reflection of continued rapid differentiation in the absence of an adequate supply of cells, may invoke an additional role for Sgk3 that is not identified in these studies.

We have uncovered Sgk3 as a new player in the anagen to catagen transition. Our results provide insight into how the transiently amplifying pool of matrix cells is maintained during the growth phase of the hair cycle, shedding light on previously unexplained observations regarding the effects of EGF and Pten on the hair cycle. The data suggest a model in which maintenance of the transiently amplifying cells is achieved by Sgk3 and possibly Pten, which act either together or separately to reduce the effects of PI3K signaling. Counterbalancing these effects are positive growth factor signals, which elevate PI3K signaling and push progenitor cell fate away from matrix maintenance and toward catagen. This work advances current understanding of how growth factor signaling regulates the anagen to catagen transition and lays the groundwork for future studies in this arena.

Materials and methods

Generation of mice lacking Sgk3

E14K ES cells from 129/Ola mice were maintained on mitomycin C–treated mouse embryonic fibroblasts in DME supplemented with leukemia inhibitory factor, 15% heat-inactivated FCS (Hyclone), L-glutamine, and β-mercaptoethanol. A 129J mouse bacterial artificial chromosome genomic library was screened with a murine Sgk3 partial cDNA probe. Restriction mapping and sequencing of subcloned fragments revealed that the murine Sgk3 gene contains 16 coding exons. The targeting vector replaced exons 8 and 9, encoding a critical part of the kinase domain, and the neomycin resistance gene was under control of the phosphoglycerate kinase (*PGK*) promoter (*PGK-neo*); stop codons were introduced downstream of the splice acceptor site of exon 8. The diphtheria toxin A gene allowed for negative selection. The targeting vector was linearized with NotI and was electroporated into ES cells (0.34 kV and 250 μF; Gene Pulser; Bio-Rad Laboratories). 768 G418–resistant ES cell clones were screened by PCR for homologous recombination; positive clones were confirmed by Southern blotting using external probe A (Fig. 1 A). Nine correctly targeted clones were identified; three were injected into C57BL/6J blastocysts, and two independent Sgk3 mutant mouse strains were established.

Genotypes of mutant mice were determined by PCR and were confirmed by Southern blotting of genomic DNA from tail biopsies using an external probe. Primers a and b detected the WT allele; primers c and d, which are specific for *neo*, detected the mutant allele. The primer sequences are listed as follows: primer a, 5′-ATTTTCCATCCAGTTTCCGTTTT -3′; primer b, 5′-CACAGCCTCGCTTCAGTATTTT-3′; primer c, 5′-GTAGTGGGGCTGTGGTGAAATAAA-3′; and primer d, 5′-CGCCTTCTATCGCCTTGAC-3′. For Northern analysis, samples were prepared from P5 whole skin using Trizol; 18 μg of total RNA was run on a formaldehyde gel in 1× MOPS, transferred to Zeta-Probe GT membrane (Bio-Rad Laboratories), and probed using ExpressHyb (BD Biosciences). For immunoblot sample preparation, keratinocytes were lysed in NP-40–radioimmunoprecipitation assay (RIPA; 50 mM Tris, pH 7.4, 150 mM NaCl, 0.5% NP-40, and 5 mM EDTA, pH 8.0). Skin fractions were obtained by dispase (Roche) treatment for 30 min at 37°C; fractions that were frozen in liquid nitrogen were smashed using a tissue smasher, resuspended in NP-40–RIPA, sonicated 3 × 20 s, spun 20 min at maximum in a tabletop centrifuge, and quantified using a Bradford-based assay. Membranes were probed using an antibody generated against the NH_2-terminal Phox domain (gift from Z. Songyang, Baylor College of Medicine, Houston, TX).

Microscopy, digital photography, and image processing

Gross images were obtained using a digital camera (model C-5060; Olympus) or a dissection scope (model MZFLIII; Leica) equipped with a camera (Axiocam; Carl Zeiss MicroImaging, Inc.) driven by Axiovision (Carl Zeiss MicroImaging, Inc.). Light and fluorescent microscopy images were obtained using a microscope (Axioskop; Carl Zeiss MicroImaging, Inc.) equipped with 40× plan-Neofluar 1.3 (Immersol 518F oil), 20× plan-Neofluar 0.5 (air), and 10× plan-Apochromat 0.45 (air) objectives (all from Carl Zeiss MicroImaging, Inc.) and were captured using a camera (Spot RT; Diagnostic Instruments) driven by Metamorph software (Molecular Devices). Scanning EM images were obtained using a field emission scanning electron microscope (model 1550; LEO Electron Microscopy, Inc.), and transmission EM images were taken with a transmission electron microscope (Tecnai G2-12; FEI) equipped with a digital camera (model XR60; Advanced Microscopy Techniques, Corp.).

Tissue histology, immunofluorescence, and EM

Skin was frozen in optimal cutting temperature compound (VWR), and 10-μM sections were cut. For alkaline phosphatase, sections were fixed in 4% PFA for 10 min at RT, reacted with BCIP/nitroblue tetrazolium in 100 mM Tris, pH 9.5, 100 mM NaCl, 50 mM $MgCl_2$, and counterstained with nuclear fast red (Vector Laboratories). For Xgal, sections were fixed for 2 min in 0.5% glutaraldehyde and reacted in 100 mM Na phosphate, pH 7.3, 1.3 mM $MgCl_2$, 3 mM $K_3Fe(CN)_6$, 3 mM $K_4Fe(CN)_6$, and 1 mM Xgal (Invitrogen). For immunofluorescence, sections were fixed 10 min in 4% PFA. For mouse mAbs, we used the MOM basic kit (Vector Laboratories); for all other antibodies, we blocked 1–4 h (2.5% normal goat serum, 2.5% normal donkey serum, 1% BSA, and 0.1% Triton X-100), incubated with primary antibody overnight at 4°C in block, fluorescence conjugated secondary antibodies (Jackson ImmunoResearch Laboratories) for 40 min at RT in block, and counterstained with DAPI. For immunohistochemistry, secondary antibodies were HRP conjugated; HRP substrate was Vector Nova-Red (Vector Laboratories), and counterstain was hematoxylin. Antibodies that were used are listed as follows: AE13 (1:50; gift from T.T. Sun, New York University, New York, NY), AE15 (1:20; gift from T.T. Sun), Lef1 (1:300; lab generated), keratin 6 (1:200; lab generated), BrdU (1:500; Abcam), activated caspase 3 (1:1,000; R&D Systems), phospho-Akt 1–3 (1:100; Cell Signaling), and EGFR (1:100; Upstate Biotechnology). For scanning EM, samples were fixed in 2% glutaraldehyde, 4% PFA, and 2 mM $CaCl_2$ in 0.05 M sodium cacodylate buffer, pH 7.2, at RT for >1 h, dehydrated, critical-point dried, mounted, and sputter coated with gold palladium. For transmission EM, samples were fixed as described for scanning EM, postfixed in 1% osmium tetroxide, and processed for Epon embedding; ultrathin sections (60–70 nm) were counterstained with uranyl acetate and lead citrate.

Quantification of cell number, apoptosis, and proliferation

For cell number, sections were stained with hematoxylin; 20 consecutive bulbs cut through the midline (determined by DP morphology) were

counted from the bottom of the bulb to the top of the DP. For apoptosis, sections were stained for activated caspase 3 and scored for the number of bulbs present and number of cells that were positive for caspase per bulb. For proliferation, mice were injected with 50 μg/g BrdU (Sigma-Aldrich) subcutaneous exactly 2 h before killing. Staining was performed as described for immunofluorescence with an additional 30-min incubation in 1 N HCl at 37°C after fixation. 50 consecutive bulbs were counted for the number of BrdU (+) nuclei. All statistical analysis was performed using Prism (GraphPad Software).

BrdU fate mapping of bulb cells

Mice injected with a single dose of 50 μg/g BrdU at P4 were killed at 4, 12, or 20 h. Sections were stained with AE13, BrdU, and DAPI. For each of three experiments, 10 bulbs per set were counted for total bulb cell number, BrdU (+) cells below the line of AE13 differentiation (defined as the lowest cell stained for AE13), and BrdU (+) cells above the line of differentiation. For counts above the level of differentiation, BrdU (+) cells external to, within, and internal to the AE13-positive cells were pooled such that counts include IRS, hair shaft, and medulla cells; ORS cells were excluded.

Keratinocyte culture and growth factor experiments

Keratinocytes that were isolated by floating newborn skin on dispase (Roche) overnight at 4°C, 0.1% trypsin (GIBCO BRL), and 40 μM filtration (BD Falcon) were grown in E medium (Rheinwald and Green, 1977) containing 0.05 mM calcium and 15% FBS. Subconfluent cells that were starved 16–24 h in E medium lacking serum were treated with 50 ng/ml IGF-1 (Sigma-Aldrich), 10 ng/ml EGF (R&D Systems), 100 nM wortmannin (Sigma-Aldrich), and/or 1 μM MEK inhibitor 444937 (Calbiochem). Lysates were collected on ice in NP-40–RIPA with protease inhibitors. Antibodies for Western blotting included phospho-MAPK (1:2,000; Sigma-Aldrich), total MAPK, phospho-Akt (Ser473; binds Akt 1–3), and total Akt (binds Akt 1–3; all 1:1,000; Cell Signaling).

We gratefully acknowledge the help and input from members of the Fuchs lab, especially Dr. Valerie Horsley and Dr. Cedric Blanpain for thoughtful advice. We appreciate the gift of Sgk3 antibody by Dr. Zhou Songyang.

E. Fuchs is an investigator of the Howard Hughes Medical Institute. This work was supported by grants from the National Institutes of Health and the Terry Fox program of the National Cancer Institute of Canada.

Submitted: 25 April 2005
Accepted: 13 July 2005

References

Blanpain, C., W.E. Lowry, A. Geoghegan, L. Polak, and E. Fuchs. 2004. Self-renewal, multipotency, and the existence of two cell populations within an epithelial stem cell niche. *Cell.* 118:635–648.

Bol, D.K., K. Kiguchi, I. Gimenez-Conti, T. Rupp, and J. DiGiovanni. 1997. Overexpression of insulin-like growth factor-1 induces hyperplasia, dermal abnormalities, and spontaneous tumor formation in transgenic mice. *Oncogene.* 14:1725–1734.

DasGupta, R., and E. Fuchs. 1999. Multiple roles for activated LEF/TCF transcription complexes during hair follicle development and differentiation. *Development.* 126:4557–4568.

Datta, S.R., A. Brunet, and M.E. Greenberg. 1999. Cellular survival: a play in three Akts. *Genes Dev.* 13:2905–2927.

Di-Poi, N., C.Y. Ng, N.S. Tan, Z. Yang, B.A. Hemmings, B. Desvergne, L. Michalik, and W. Wahli. 2005. Epithelium-mesenchyme interactions control the activity of peroxisome proliferator-activated receptor beta/delta during hair follicle development. *Mol. Cell. Biol.* 25:1696–1712.

DiGiovanni, J., D.K. Bol, E. Wilker, L. Beltran, S. Carbajal, S. Moats, A. Ramirez, J. Jorcano, and K. Kiguchi. 2000. Constitutive expression of insulin-like growth factor-1 in epidermal basal cells of transgenic mice leads to spontaneous tumor promotion. *Cancer Res.* 60:1561–1570.

Firestone, G.L., J.R. Giampaolo, and B.A. O'Keeffe. 2003. Stimulus-dependent regulation of serum and glucocorticoid inducible protein kinase (SGK) transcription, subcellular localization and enzymatic activity. *Cell. Physiol. Biochem.* 13:1–12.

Guo, L., L. Degenstein, and E. Fuchs. 1996. Keratinocyte growth factor is required for hair development but not for wound healing. *Genes Dev.* 10:165–175.

Hansen, L.A., N. Alexander, M.E. Hogan, J.P. Sundberg, A. Dlugosz, D.W. Threadgill, T. Magnuson, and S.H. Yuspa. 1997. Genetically null mice reveal a central role for epidermal growth factor receptor in the differentiation of the hair follicle and normal hair development. *Am. J. Pathol.* 150:1959–1975.

Hebert, J.M., T. Rosenquist, J. Gotz, and G.R. Martin. 1994. FGF5 as a regulator of the hair growth cycle: evidence from targeted and spontaneous mutations. *Cell.* 78:1017–1025.

Holbro, T., G. Civenni, and N.E. Hynes. 2003. The ErbB receptors and their role in cancer progression. *Exp. Cell Res.* 284:99–110.

Hollis, D.E., and R.E. Chapman. 1987. Apoptosis in wool follicles during mouse epidermal growth factor (mEGF)-induced catagen regression. *J. Invest. Dermatol.* 88:455–458.

Hollis, D.E., R.E. Chapman, B.A. Panaretto, and G.P. Moore. 1983. Morphological changes in the skin and wool fibres of Merino sheep infused with mouse epidermal growth factor. *Aust. J. Biol. Sci.* 36:419–434.

Johnson, G.L., and R. Lapadat. 2002. Mitogen-activated protein kinase pathways mediated by ERK, JNK, and p38 protein kinases. *Science.* 298:1911–1912.

Karlsson, L., C. Bondjers, and C. Betsholtz. 1999. Roles for PDGF-A and sonic hedgehog in development of mesenchymal components of the hair follicle. *Development.* 126:2611–2621.

Kobayashi, T., and P. Cohen. 1999. Activation of serum- and glucocorticoid-regulated protein kinase by agonists that activate phosphatidylinositide 3-kinase is mediated by 3-phosphoinositide-dependent protein kinase-1 (PDK1) and PDK2. *Biochem. J.* 339:319–328.

Kobayashi, T., M. Deak, N. Morrice, and P. Cohen. 1999. Characterization of the structure and regulation of two novel isoforms of serum- and glucocorticoid-induced protein kinase. *Biochem. J.* 344:189–197.

Lang, F., and P. Cohen. 2001. Regulation and physiological roles of serum- and glucocorticoid-induced protein kinase isoforms. *Sci. STKE.* 10.1126/stke.2001.108.re17.

Lehrer, M.S., T.T. Sun, and R.M. Lavker. 1998. Strategies of epithelial repair: modulation of stem cell and transit amplifying cell proliferation. *J. Cell Sci.* 111:2867–2875.

Liu, J.P., J. Baker, A.S. Perkins, E.J. Robertson, and A. Efstratiadis. 1993. Mice carrying null mutations of the genes encoding insulin-like growth factor I (Igf-1) and type 1 IGF receptor (Igf1r). *Cell.* 75:59–72.

Liu, D., X. Yang, and Z. Songyang. 2000. Identification of CISK, a new member of the SGK kinase family that promotes IL-3-dependent survival. *Curr. Biol.* 10:1233–1236.

McCormick, J.A., Y. Feng, K. Dawson, M.J. Behne, B. Yu, J. Wang, A.W. Wyatt, G. Henke, F. Grahammer, T.M. Mauro, et al. 2004. Targeted disruption of the protein kinase SGK3/CISK impairs postnatal hair follicle development. *Mol. Biol. Cell.* 15:4278–4288.

Moore, G.P., B.A. Panaretto, and D. Robertson. 1981. Effects of epidermal growth factor on hair growth in the mouse. *J. Endocrinol.* 88:293–299.

Moore, G.P., B.A. Panaretto, and D. Robertson. 1982. Inhibition of wool growth in merino sheep following administration of mouse epidermal growth factor and a derivative. *Aust. J. Biol. Sci.* 35:163–172.

Morris, R.J., Y. Liu, L. Marles, Z. Yang, C. Trempus, S. Li, J.S. Lin, J.A. Sawicki, and G. Cotsarelis. 2004. Capturing and profiling adult hair follicle stem cells. *Nat. Biotechnol.* 22:411–417.

Muller-Rover, S., B. Handjiski, C. van der Veen, S. Eichmuller, K. Foitzik, I.A. McKay, K.S. Stenn, and R. Paus. 2001. A comprehensive guide for the accurate classification of murine hair follicles in distinct hair cycle stages. *J. Invest. Dermatol.* 117:3–15.

Murillas, R., F. Larcher, C.J. Conti, M. Santos, A. Ullrich, and J.L. Jorcano. 1995. Expression of a dominant negative mutant of epidermal growth factor receptor in the epidermis of transgenic mice elicits striking alterations in hair follicle development and skin structure. *EMBO J.* 14:5216–5223.

Oshima, H., A. Rochat, C. Kedzia, K. Kobayashi, and Y. Barrandon. 2001. Morphogenesis and renewal of hair follicles from adult multipotent stem cells. *Cell.* 104:233–245.

Peng, X.D., P.Z. Xu, M.L. Chen, A. Hahn-Windgassen, J. Skeen, J. Jacobs, D. Sundararajan, W.S. Chen, S.E. Crawford, K.G. Coleman, and N. Hay. 2003. Dwarfism, impaired skin development, skeletal muscle atrophy, delayed bone development, and impeded adipogenesis in mice lacking Akt1 and Akt2. *Genes Dev.* 17:1352–1365.

Philpott, M.P., D.A. Sanders, and T. Kealey. 1994. Effects of insulin and insulin-like growth factors on cultured human hair follicles: IGF-I at physiologic concentrations is an important regulator of hair follicle growth in vitro. *J. Invest. Dermatol.* 102:857–861.

Rheinwald, J.G., and H. Green. 1977. Epidermal growth factor and the multiplication of cultured human epidermal keratinocytes. *Nature*. 265:421–424.

Rosenquist, T.A., and G.R. Martin. 1996. Fibroblast growth factor signalling in the hair growth cycle: expression of the fibroblast growth factor receptor and ligand genes in the murine hair follicle. *Dev. Dyn.* 205:379–386.

Schmidt-Ullrich, R., and R. Paus. 2005. Molecular principles of hair follicle induction and morphogenesis. *Bioessays.* 27:247–261.

Stenn, K.S., and R. Paus. 2001. Controls of hair follicle cycling. *Physiol. Rev.* 81:449–494.

Su, H.Y., J.G. Hickford, R. Bickerstaffe, and B.R. Palmer. 1999a. Insulin-like

growth factor 1 and hair growth. *Dermatol. Online J.* 5:1.

Su, H.Y., J.G. Hickford, P.H. The, A.M. Hill, C.M. Frampton, and R. Bickerstaffe. 1999b. Increased vibrissa growth in transgenic mice expressing insulin-like growth factor 1. *J. Invest. Dermatol.* 112:245–248.

Sulis, M.L., and R. Parsons. 2003. PTEN: from pathology to biology. *Trends Cell Biol.* 13:478–483.

Sundberg, J.P., M.H. Rourk, D. Boggess, M.E. Hogan, B.A. Sundberg, and A.P. Bertolino. 1997. Angora mouse mutation: altered hair cycle, follicular dystrophy, phenotypic maintenance of skin grafts, and changes in keratin expression. *Vet. Pathol.* 34:171–179.

Suzuki, A., S. Itami, M. Ohishi, K. Hamada, T. Inoue, N. Komazawa, H. Senoo, T. Sasaki, J. Takeda, M. Manabe, et al. 2003. Keratinocyte-specific Pten deficiency results in epidermal hyperplasia, accelerated hair follicle morphogenesis and tumor formation. *Cancer Res.* 63:674–681.

Taylor, G., M.S. Lehrer, P.J. Jensen, T.T. Sun, and R.M. Lavker. 2000. Involvement of follicular stem cells in forming not only the follicle but also the epidermis. *Cell.* 102:451–461.

van Genderen, C., R.M. Okamura, I. Farinas, R.G. Quo, T.G. Parslow, L. Bruhn, and R. Grosschedl. 1994. Development of several organs that require inductive epithelial-mesenchymal interactions is impaired in LEF-1-deficient mice. *Genes Dev.* 8:2691–2703.

Virbasius, J.V., X. Song, D.P. Pomerleau, Y. Zhan, G.W. Zhou, and M.P. Czech. 2001. Activation of the Akt-related cytokine-independent survival kinase requires interaction of its phox domain with endosomal phosphatidylinositol 3-phosphate. *Proc. Natl. Acad. Sci. USA.* 98:12908–12913.

Wilker, E., D. Bol, K. Kiguchi, T. Rupp, L. Beltran, and J. DiGiovanni. 1999. Enhancement of susceptibility to diverse skin tumor promoters by activation of the insulin-like growth factor-1 receptor in the epidermis of transgenic mice. *Mol. Carcinog.* 25:122–131.

Xu, J., D. Liu, G. Gill, and Z. Songyang. 2001. Regulation of cytokine-independent survival kinase (CISK) by the Phox homology domain and phosphoinositides. *J. Cell Biol.* 154:699–705.

Zhou, P., C. Byrne, J. Jacobs, and E. Fuchs. 1995. Lymphoid enhancer factor 1 directs hair follicle patterning and epithelial cell fate. *Genes Dev.* 9:700–713.